ACS Energy LETTERS

Open Access

http://pubs.acs.org/journal/aelccp

Energy Express

Bandgap Tunable Two-Step Vapor-Deposited Perovskite Absorbers for Perovskite-Silicon Tandem Solar Cells

Austin G. Kuba,* Kerem Artuk, Mostafa Othman, Deniz Turkay, Chiara Ongaro, Michele Debastiani, Quentin Guesnay, Mohammad Reza Golobostanfard, Maryamsadat Heydarian, Oliver Fischer, Martin C. Schubert, Florent Sahli, Yohann Ansel, Quentin Jeangros, Aïcha Hessler-Wyser, Christophe Ballif, and Christian M. Wolff*

Cite This: *ACS Energy Lett.* 2026, 11, 3164−3167

Read Online

ACCESS | Metrics & More | Article Recommendations | Supporting Information

ABSTRACT: We report a two-step thermal evaporation−close space sublimation deposition method for tunable bandgap lead halide perovskites with single junction solar cell efficiencies exceeding 20%. These absorbers are integrated into perovskite−silicon tandem solar cells with stabilized efficiencies of >29%.

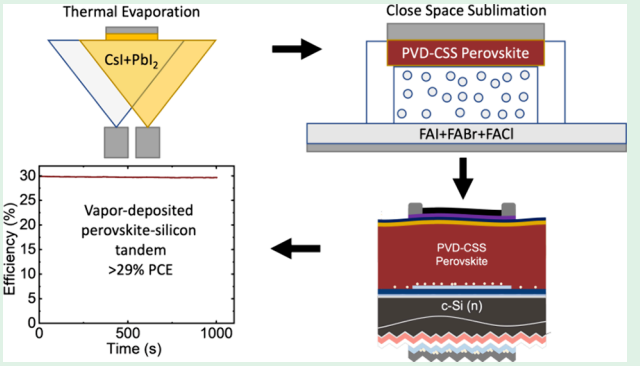

Photovoltaic energy generation continues to drive down the cost of electricity. As single junction (SJ) silicon solar cells approach their practical limits,[1] next generation concepts are needed for continued progress. The most successful route to overcoming these limits is the use of multijunction solar cells.[2,3] Perovskite−silicon tandem solar cells (TSCs) have recently seen a dramatic rise in power conversion efficiency (PCE), achieving up to 34.9%.[2] Lead halide perovskites (LHPs) have continued their progress in stability to the point that encapsulated devices can pass damp heat and have improved in accelerated aging tests[4] meaning they may soon find broader adoption in the market. However, most available reports focus on solution processes, which are still under debate regarding their suitability for commercialization on an industrial scale. Despite being rare in the literature, vapor-processed LHPs have shown promise regarding scalability and stability.[5,6] They have also attained ∼26% PCE[7] in SJ solar cells, approaching their solution-processed counterparts. However, there are still few reports of TSCs produced with fully vapor-processed LHP absorbers.[8−11] A recent breakthrough in coevaporated LHP processing has achieved >30% stabilized PCE[12] but two-step vapor-processed TSCs are still limited to <27%[11,13] to date. One technique receiving increasing attention is two-step physical-vapor-deposition close-space-sublimation (PVD-CSS, Supporting Note 1). We recently reported a PVD-CSS process capable of creating p-i-n solar cells with a broad range of bandgaps and SJ devices with efficiencies approaching 17%.[14] In this process, an inorganic lead halide-cesium halide template is deposited using thermal evaporation and then converted to a LHP by reaction with mixed organohalide vapors in a CSS configuration (Supporting Note 2). Here, we adapt this process, show the absorbers are compatible with standard passivation treatments, and incorporate these absorbers into LHP-silicon TSCs achieving >29% PCE from stabilized maximum power point (MPP) tracking.

First, a series of additives were screened. FACl produced the highest photoluminescence (PL) quantum yield (Figure S1) and has already shown promise in CSS reactions using pure formamidimium iodide (FAI)[11] so it was chosen for the rest of the work. Next, the bandgap tunability was investigated by varying the ratio of FAI to formamidinium bromide (FABr) with a constant formamidinium chloride (FACl) addition using coevaporated $CsI:PbI_2$ or $CsBr:PbI_2$ templates. The achievable range of bandgaps is shown in Figure 1a. The bandgap shows excellent tunability from 1.55 to 1.90 eV, even using pure iodide templates (spectrophotometry and PL in Figure S2). The conversion time was set to 20 min at 175 °C, and the organohalide mass addition was tuned to optimize

Received: January 16, 2026
Revised: February 15, 2026
Accepted: February 23, 2026
Published: March 13, 2026

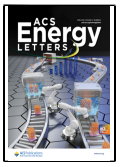

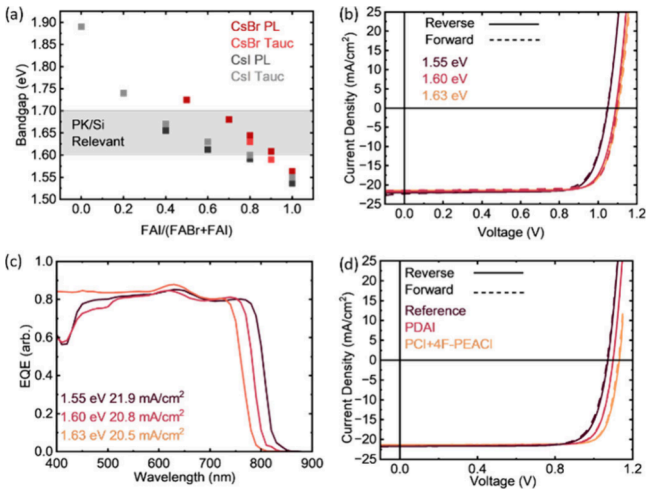

Figure 1. (a) Bandgap tunability for varying Cs source (CsI vs CsBr) with varying values of FAI/(FAI+FABr). (b) JV and (c) EQE for devices with varying bandgaps achieved by using CsI in the template and varying FAI/(FAI+FABr) from 1.0 to 0.8 to 0.6 by mass. (d) Study of surface passivation for the 1.60 eV absorber.

conversion and device performance (Figures S3 and S4). SJ solar cells with an area of 0.1 cm^2 were made with CsI:PbI_2 templates and FAI/(FAI+FABr) values of 1.0, 0.8, and 0.6 (by mass, see Supporting Note 3). The current density−voltage (JV) performance is shown in Figure 1b (JV parameters are given in Table S1). External quantum efficiency (EQE) is shown in Figure 1c. X-ray diffraction (XRD) is shown in Figure S5 and scanning electron micrographs (SEMs) are shown in Figure S6.

The 1.60 eV absorber with a short circuit current density of ∼ 21 mA/cm^2 was selected for further testing and integration into TSCs. This was expected to create good current matching with a slight bottom cell limitation based on our previous work showing a cumulative current density of 40−41 mA/cm^2 in LHP-silicon TSCs with flat front, rear textured silicon bottom cells.[15] SJ devices incorporating no passivation, propane-1,3-diammonium iodide ($PDAI_2$),[16] or bimolecular passivation of 4F-phenylethylammonium chloride (4F-PEACl) and piperazinium chloride (PCl)[17] are shown in Figure 1d, with bimolecular passivation achieving a champion efficiency of >20% without optical management. Across two batches of six films with different passivation conditions, excellent repeatability and yield were shown (Figure S7).

Six LHP-silicon TSCs with an active area of 1 cm^2 were made with $PDAI_2$ passivation. Good consistency across the batch was shown, with a mean PCE of 29.1% ± 0.6 (n = 6, average of forward and reverse scans) and a minimum of 27.8%. Cross-section SEM is shown in Figure 2a and (top-view Figure S8), and a schematic of the devices is shown in Figure 2b. The champion device reached 30.7% PCE from the reverse JV scan (Figure 2c) with a MPP efficiency of 29.8% for the first 300 s and minor degradation to 29.7% over 1000 s of tracking unencapsulated in air (Figure 2d). The champion device also showed good shelf stability, retaining 99% of its MPP efficiency over 134 days of storage in a N_2 environment (Figure S9). Subcell selective EQE of the champion device is shown in Figure 2e. Current mismatch measurements confirm that the top cell produces 1 mA/cm^2 more than the bottom cell (Figure S10) which can be improved for marginal current gains by increasing the FABr:FAI ratio to fine-tune the LHP bandgap. Four of the TSCs were cross-tested at Fraunhofer ISE after 3 weeks of shelf storage for an independent confirmation of the device performance. The JV parameters of the champion device and the selected devices are given in Table S2 and Figure S11 at both institutes. The relative error in the PCE for the champion device is 2% from MPP tracking (Figure S12). Subcell selective PL-based iV_{OC} images[18] (Figure 2f,g) of the champion TSC show good uniformity with small point-like defects in the top cell and an average iV_{oc} of 1.158 V for the top cell and 0.724 V from the bottom cell, in good agreement with the measured V_{oc} from JV. To explore the suitability of this process for TSCs on textured silicon bottom cells, we made one batch of LHP-silicon TSCs on textured Si with pyramid sizes ∼1 μm (SEM shown in Figure S13). The champion device achieved a maximum PCE of 28.3% from

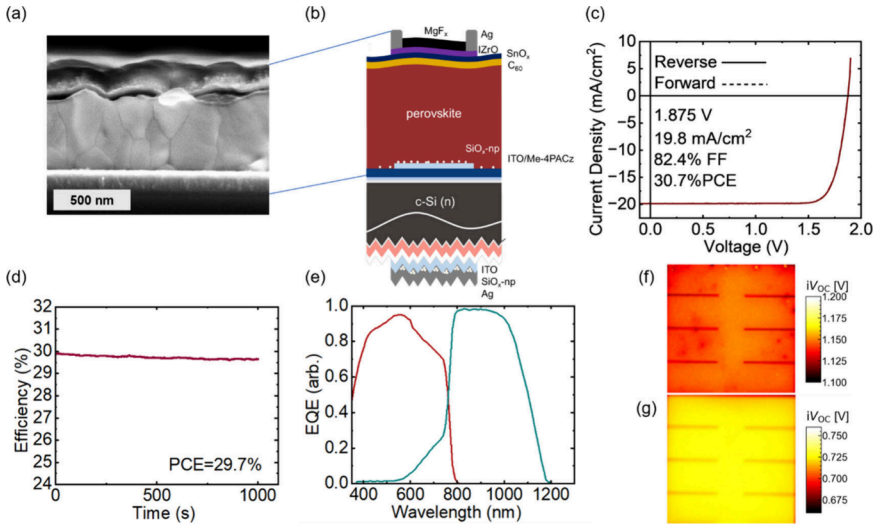

Figure 2. (a) Cross section SEM of a LHP-silicon tandem device produced in this work focused on the LHP top cell. (b) Schematic of a tandem device. (c) JV curve of the champion tandem solar cell produced in this work. (d) MPP tracking of the champion device for 1000 s unencapsulated in air. (e) Subcell selective EQE for the top and bottom cell. (f) Subcell selective PL-based iV_{OC} images of the LHP top cell and (g) silicon bottom cell (full image width 1 cm in both cases).

https://doi.org/10.1021/acsenergylett.6c00156
ACS Energy Lett. 2026, 11, 3164−3167

reverse JV (Figure S14) with V_{oc} = 1.86 V and J_{sc} = 20.4 mA/cm^2 but low FF = 75%. Sister devices on ohmic textured Si substrates show that the low FF is likely related to low shunt resistance (Figure S14), which must be improved in future work to enable high efficiency textured TSCs.

In conclusion, we report the fabrication of two-step vapor-deposited LHP-silicon tandem solar cells with good scalability potential and efficiencies >29% through a PVD-CSS process. This report represents a significant advance in the performance of two-step vapor-deposited LHP-silicon tandem solar cells. These results motivate further studies into the potential advantages or disadvantages that vapor-deposited LHPs may have, in terms of stability and scalability, for both single junction and multijunction solar cells, and whether their efficiencies can further approach solution-processed solar cells in record efficiency.

■ ASSOCIATED CONTENT

Supporting Information

The Supporting Information is available free of charge at https://pubs.acs.org/doi/10.1021/acsenergylett.6c00156.

Experimental details and additional data on LHP films, single junction, and tandem solar cells (PDF)

■ AUTHOR INFORMATION

Corresponding Authors

Austin G. Kuba − *Ecole Polytechnique Fédérale de Lausanne (EPFL), Institute of Electrical and Microengineering (IEM), Photovoltaics and Thin-Film Electronics Laboratory, 2000 Neuchâtel, Switzerland;* orcid.org/0000-0001-6500-2646; Email: agkuba@gmail.com

Christian M. Wolff − *Ecole Polytechnique Fédérale de Lausanne (EPFL), Institute of Electrical and Microengineering (IEM), Photovoltaics and Thin-Film Electronics Laboratory, 2000 Neuchâtel, Switzerland;* orcid.org/0000-0002-7210-1869; Email: christian.wolff@epfl.ch

Authors

Kerem Artuk − *Ecole Polytechnique Fédérale de Lausanne (EPFL), Institute of Electrical and Microengineering (IEM), Photovoltaics and Thin-Film Electronics Laboratory, 2000 Neuchâtel, Switzerland*

Mostafa Othman − *Ecole Polytechnique Fédérale de Lausanne (EPFL), Institute of Electrical and Microengineering (IEM), Photovoltaics and Thin-Film Electronics Laboratory, 2000 Neuchâtel, Switzerland;* orcid.org/0000-0001-6987-0176

Deniz Turkay − *Ecole Polytechnique Fédérale de Lausanne (EPFL), Institute of Electrical and Microengineering (IEM), Photovoltaics and Thin-Film Electronics Laboratory, 2000 Neuchâtel, Switzerland;* orcid.org/0000-0002-8522-6919

Chiara Ongaro − *Ecole Polytechnique Fédérale de Lausanne (EPFL), Institute of Electrical and Microengineering (IEM), Photovoltaics and Thin-Film Electronics Laboratory, 2000 Neuchâtel, Switzerland*

Michele Debastiani − *Centre Suisse d'Electronique et de Microtechnique (CSEM), 2002 Neuchâtel, Switzerland*

Quentin Guesnay − *Ecole Polytechnique Fédérale de Lausanne (EPFL), Institute of Electrical and Microengineering (IEM), Photovoltaics and Thin-Film Electronics Laboratory, 2000 Neuchâtel, Switzerland*

Mohammad Reza Golobostanfard − *Ecole Polytechnique Fédérale de Lausanne (EPFL), Institute of Electrical and Microengineering (IEM), Photovoltaics and Thin-Film Electronics Laboratory, 2000 Neuchâtel, Switzerland; Smart Energy Materials, Department of Chemistry, University of Turku, 20500 Turku, Finland*

Maryamsadat Heydarian − *Fraunhofer Institute for Solar Energy Systems, 79110 Freiburg, Germany;* orcid.org/0000-0002-4053-0888

Oliver Fischer − *Fraunhofer Institute for Solar Energy Systems, 79110 Freiburg, Germany; Chair for Photovoltaic energy Conversion, Department of Sustainable Systems Engineering INATECH, University of Freiburg, 79110 Freiburg, Germany;* orcid.org/0009-0006-9544-4246

Martin C. Schubert − *Fraunhofer Institute for Solar Energy Systems, 79110 Freiburg, Germany*

Florent Sahli − *Centre Suisse d'Electronique et de Microtechnique (CSEM), 2002 Neuchâtel, Switzerland*

Yohann Ansel − *Centre Suisse d'Electronique et de Microtechnique (CSEM), 2002 Neuchâtel, Switzerland*

Quentin Jeangros − *Centre Suisse d'Electronique et de Microtechnique (CSEM), 2002 Neuchâtel, Switzerland*

Aïcha Hessler-Wyser − *Ecole Polytechnique Fédérale de Lausanne (EPFL), Institute of Electrical and Microengineering (IEM), Photovoltaics and Thin-Film Electronics Laboratory, 2000 Neuchâtel, Switzerland*

Christophe Ballif − *Ecole Polytechnique Fédérale de Lausanne (EPFL), Institute of Electrical and Microengineering (IEM), Photovoltaics and Thin-Film Electronics Laboratory, 2000 Neuchâtel, Switzerland*

Complete contact information is available at: https://pubs.acs.org/10.1021/acsenergylett.6c00156

Notes

The authors declare no competing financial interest.

■ ACKNOWLEDGMENTS

The authors acknowledge funding from the European Union's Horizon 2020 research and innovation program (TRIUMPH, 101075725), the Swiss State Secretariat for Education Research and Innovation (SERI) (TRIUMPH, 101075725), the Swiss Federal Office of Energy (PERSISTARS, BESTO-BOT), the "fonds électricité vitale vert des Services industriels de Genèves", and the ETH Domain through an AM grant (AMYS). M.O., D.T., and A.G.K. acknowledge funding from the European Union's Horizon 2020 research and innovation program under a Marie Skłodowska-Curie grant (945363 and 101034260). D.T. acknowledges the State Secretariat for Education, Research, and Innovation for an FCS/ESKAS Swiss Government Excellence Scholarship.

■ REFERENCES

(1) Green, M. A. Limits on the Open-Circuit Voltage and Efficiency of Silicon Solar Cells Imposed by Intrinsic Auger Processes. *IEEE Trans. Electron Devices* **1984**, *31* (5), 671−678.

(2) Green, M. A.; Dunlop, E. D.; Yoshita, M.; Kopidakis, N.; Bothe, K.; Siefer, G.; Hao, X.; Jiang, J. Y. Solar Cell Efficiency Tables (Version 66). *Prog. Photovolt. Res. Appl.* **2025**, *33* (7), 795−810.

(3) Hörantner, M. T.; Leijtens, T.; Ziffer, M. E.; Eperon, G. E.; Christoforo, M. G.; McGehee, M. D.; Snaith, H. J. The Potential of Multijunction Perovskite Solar Cells. *ACS Energy Lett.* **2017**, *2* (10), 2506−2513.

(4) Zhu, H.; Teale, S.; Lintangpradipto, M. N.; Mahesh, S.; Chen, B.; McGehee, M. D.; Sargent, E. H.; Bakr, O. M. Long-Term Operating Stability in Perovskite Photovoltaics. *Nat. Rev. Mater.* **2023**, *8* (9), 569−586.
(5) Abzieher, T.; Moore, D. T.; Roß, M.; Albrecht, S.; Silvia, J.; Tan, H.; Jeangros, Q.; Ballif, C.; Hoerantner, M. T.; Kim, B.-S.; Bolink, H. J.; Pistor, P.; Goldschmidt, J. C.; Chiang, Y.-H.; Stranks, S. D.; Borchert, J.; McGehee, M. D.; Morales-Masis, M.; Patel, J. B.; Bruno, A.; Paetzold, U. W. Vapor Phase Deposition of Perovskite Photovoltaics: Short Track to Commercialization? *Energy Environ. Sci.* **2024**, *17* (5), 1645−1663.
(6) Huang, L.; Chen, Z.; Wang, K.; Wang, Z. Dry-Processed Perovskite Photovoltaics: Materials, Fabrication Techniques, and Devices. *Adv. Energy Mater.* **2025**, *15* (47), No. e03501.
(7) Zhou, J.; Tan, L.; Liu, Y.; Li, H.; Liu, X.; Li, M.; Wang, S.; Zhang, Y.; Jiang, C.; Hua, R.; Tress, W.; Meloni, S.; Yi, C. Highly Efficient and Stable Perovskite Solar Cells via a Multifunctional Hole Transporting Material. *Joule* **2024**, *8* (6), 1691−1706.
(8) Roß, M.; Severin, S.; Stutz, M. B.; Wagner, P.; Köbler, H.; Favin-Lévêque, M.; Al-Ashouri, A.; Korb, P.; Tockhorn, P.; Abate, A.; Stannowski, B.; Rech, B.; Albrecht, S. Co-Evaporated Formamidinium Lead Iodide Based Perovskites with 1000 h Constant Stability for Fully Textured Monolithic Perovskite/Silicon Tandem Solar Cells. *Adv. Energy Mater.* **2021**, *11* (35), 2101460−2101460.
(9) Xu, Y.; Jiang, Y.; Du, H.; Gao, X.; Qiang, Z.; Wang, C.; Tao, Z.; Yang, L.; Zhi, R.; Liang, G.; Cai, H.; Rothmann, M. U.; Cheng, Y.; Li, W. Octahedral Tilt Enables Efficient and Stable Fully Vapor-Deposited Perovskite/Silicon Tandem Cells. *Adv. Funct. Mater.* **2024**, *34* (11), No. 2312037.
(10) Chozas-Barrientos, S.; Paliwal, A.; Ventosinos, F.; Roldán-Carmona, C.; Gil-Escrig, L.; Held, V.; Carroy, P.; Muñoz, D.; Bolink, H. J. Molecular Recombination Junction for Vacuum-Deposited Perovskite/Silicon Two-Terminal Tandem Solar Cells. *ACS Energy Lett.* **2025**, *10* (4), 1733−1740.
(11) Zhang, Y.; Zhu, Y.; Sun, J.; Hu, M.; Chen, J.; Duan, B.; Hu, S.; Hou, P.; Tan, W. L.; Ku, Z.; Yang, W.; Lu, J. Low Pressure Chemical Vapor Deposited Perovskite Enables All Vacuum-Processed Monolithic Perovskite-Silicon Tandem Solar Cells. *Adv. Energy Mater.* **2025**, *15* (27), No. 2405377.
(12) Li, N.; Niu, X.; Dong, Z.; Hu, J.; Luo, R.; Yang, S.; Zhou, Q.; Shi, Z.; Chen, J.; Du, X.; Lee, L. K.; Wang, Y.; Guo, X.; Wang, X.; Qiu, C.-W.; Lin, M.; He, R.; Zhang, X.; Chen, Y.; Wu, M.; Hou, Y. Optimal Perovskite Vapor Partitioning on Textured Silicon for High-Stability Tandem Solar Cells. *Science.* **2025**, *390*, 6779.
(13) Mahboubi Soufiani, A.; Moumine, H.; Wutke, E.; Farias Basulto, G. A.; De Araujo, W. M. B.; Leyden, M.; Szot, M.; Bertram, T.; Škorjanc, V.; Harter, A.; Severin, S.; Roß, M.; Mainz, R.; Schlatmann, R.; Albrecht, S.; Stannowski, B.; Kurpiers, J. Sequentially Evaporated Wide Bandgap Perovskite Absorber for Large-Area and Reproducible Fabrication of Solar Cells. *Sol. RRL* **2025**, *9* (19), No. 2500412.
(14) Guesnay, Q.; Sahli, F.; Artuk, K.; Turkay, D.; Kuba, A. G.; Mrkyvkova, N.; Vegso, K.; Siffalovic, P.; Schreiber, F.; Lai, H.; Fu, F.; Ledinský, M.; Fürst, N.; Schafflützel, A.; Bucher, C.; Jeangros, Q.; Ballif, C.; Wolff, C. M. Pizza Oven Processing of Organohalide Perovskites (POPOP): A Simple, Versatile and Efficient Vapor Deposition Method. *Adv. Energy Mater.* **2024**, *14* (10), No. 2303423.
(15) Turkay, D.; Artuk, K.; Chin, X.-Y.; Jacobs, D. A.; Moon, S.-J.; Walter, A.; Mensi, M.; Andreatta, G.; Blondiaux, N.; Lai, H.; Fu, F.; Boccard, M.; Jeangros, Q.; Wolff, C. M.; Ballif, C. Synergetic Substrate and Additive Engineering for over 30%-Efficient Perovskite-Si Tandem Solar Cells. *Joule* **2024**, *8* (6), 1735−1753.
(16) Chen, H.; Maxwell, A.; Li, C.; Teale, S.; Chen, B.; Zhu, T.; Ugur, E.; Harrison, G.; Grater, L.; Wang, J.; Wang, Z.; Zeng, L.; Park, S. M.; Chen, L.; Serles, P.; Awni, R. A.; Subedi, B.; Zheng, X.; Xiao, C.; Podraza, N. J.; Filleter, T.; Liu, C.; Yang, Y.; Luther, J. M.; De Wolf, S.; Kanatzidis, M. G.; Yan, Y.; Sargent, E. H. Regulating Surface Potential Maximizes Voltage in All-Perovskite Tandems. *Nature* **2023**, *613* (7945), 676−681.
(17) Artuk, K.; Turkay, D.; Kuba, A. G.; Riemelmoser, S.; Steele, J.; Quest, H.; De Bastiani, M.; Diekmann, J.; Hurni, J.; Ongaro, C.; Othman, M.; Heydarian, M.; Fischer, O.; Lai, H.; Zeiske, S.; López-Arteaga, R.; Mensi, M. D.; Saenz, F.; Champault, L.; Can, H. A.; Golobostanfard, M. R.; Desai, U.; Remondeau, P.; Solano, E.; Faes, A.; Fu, F.; Schubert, M.; Schindler, F.; Chen, B.; Pasquarello, A.; Sargent, E.; Hessler-Wyser, A.; Portale, G.; Jeangros, Q.; Ballif, C.; Wolff, C. Perovskite-Perovskite-Silicon Triple Junction Solar Cells with Improved Carrier and Photon Management. *Resesarch Square*, Submitted 2025−08−05. **2025**na (accessed 2025−08−06).
(18) Fischer, O.; Bui, A. D.; Schindler, F.; Macdonald, D.; Glunz, S. W.; Nguyen, H. T.; Schubert, M. C. Versatile Implied Open-circuit Voltage Imaging Methods and Its Application in Monolithic Tandem Solar Cells. *Prog. Photovolt. Res. Appl.* **2025**, *33* (1), 40−53.

NOTE ADDED AFTER ASAP PUBLICATION

The version of this paper that was published ASAP March 13, 2026, contained a spelling error in the name of author Mohammad Reza Golobostanfard. The corrected version posted March 18, 2026.

https://doi.org/10.1021/acsenergylett.6c00156
ACS Energy Lett. 2026, 11, 3164−3167